MCB
Journals.ASM.org

Oxidative Processing of Latent Fas in the Endoplasmic Reticulum Controls the Strength of Apoptosis

Vikas Anathy,[a] Elle Roberson,[a] Brian Cunniff,[a] James D. Nolin,[a] Sidra Hoffman,[a] Page Spiess,[a] Amy S. Guala,[a] Karolyn G. Lahue,[a] Dylan Goldman, Stevenson Flemer,[b] Albert van der Vliet,[a] Nicholas H. Heintz,[a] Ralph C. Budd,[c] Kenneth D. Tew,[d] and Yvonne M. W. Janssen-Heininger[a]

Departments of Pathology,[a] Chemistry,[b] and Medicine,[c] University of Vermont, Burlington, Vermont, USA, and Department of Cell and Molecular Pharmacology, Medical University of South Carolina, Charleston, South Carolina, USA[d]

We recently demonstrated that S-glutathionylation of the death receptor Fas (Fas-SSG) amplifies apoptosis (V. Anathy et al., J. Cell Biol. 184:241–252, 2009). In the present study, we demonstrate that distinct pools of Fas exist in cells. Upon ligation of surface Fas, a separate pool of latent Fas in the endoplasmic reticulum (ER) underwent rapid oxidative processing characterized by the loss of free sulfhydryl content (Fas-SH) and resultant increases in S-glutathionylation of Cys294, leading to increases of surface Fas. Stimulation with FasL rapidly induced associations of Fas with ERp57 and glutathione *S*-transferase π (GSTP), a protein disulfide isomerase and catalyst of S-glutathionylation, respectively, in the ER. Knockdown or inhibition of ERp57 and GSTP1 substantially decreased FasL-induced oxidative processing and S-glutathionylation of Fas, resulting in decreased death-inducing signaling complex formation and caspase activity and enhanced survival. Bleomycin-induced pulmonary fibrosis was accompanied by increased interactions between Fas-ERp57-GSTP1 and S-glutathionylation of Fas. Importantly, fibrosis was largely prevented following short interfering RNA-mediated ablation of ERp57 and GSTP. Collectively, these findings illuminate a regulatory switch, a ligand-initiated oxidative processing of latent Fas, that controls the strength of apoptosis.

Fas (CD95 or Apo-1) is a constitutively expressed member of the tumor necrosis factor (TNF) receptor (TNFR) superfamily of death receptors that share a conserved 80-amino-acid death domain in their cytoplasmic tails that is critical in apoptosis signaling (18). Upon ligation of Fas, the sequential association of FADD and procaspase forms of caspase-8 or -10 leads to the formation of the death-inducing signaling complex (DISC), resulting in the activation of caspase-8 or -10 and execution of apoptosis (18). We have recently demonstrated that Fas can be posttranslationally modified in a redox-dependent manner via the covalent attachment of the small antioxidant tripeptide, glutathione (GSH). This posttranslational modification is known as protein S-glutathionylation (SSG). S-glutathionylation of cysteine 294 in the endodomain of murine Fas (Fas-SSG) was sustained via caspase-dependent degradation of the deglutathionylating enzyme, glutaredoxin-1 (Grx1). Fas-SSG was shown to be functionally important, as it enhances recruitment of Fas into lipid rafts and promotes FasL binding, DISC formation, and caspase activation, thereby amplifying cell death (3). Despite these novel observations, the early events that mediate S-glutathionylation of Fas remain unknown.

ERp57 (PDIA3) belongs to the protein disulfide isomerase (PDI; EC 5.3.4.1) family of oxidoreductases that primarily localize in the endoplasmic reticulum (ER) and catalyze intramolecular disulfide bond (S-S) formation in proteins to fold into their active/native conformation (11). While catalyzing disulfide bonds, the recycling phase of PDI enzymes is known to produce the oxidant H_2O_2 (48, 53), and accumulation of H_2O_2 can lead to protein S-glutathionylation (33, 37). Crystallographic evidence and three-dimensional (3D) structure predictions suggest that ectodomain cysteines of TNF receptor family members are in intermolecular disulfide bonds and are essential for ligand binding activity (7, 42). However, no reports exist to date that document interaction of Fas or any TNF receptors with PDI family enzymes in order to form disulfide bridges.

Glutathione *S*-transferases (GST; EC 2.5.1.18) are classically known as phase II detoxifying enzymes that catalyze the conjugation of GSH to various electrophilic molecules (9, 13). Recent reports demonstrate that GSTP1 can catalyze protein S-glutathionylation following oxidative and nitrosative stress (47), and that GSTP-catalyzed S-glutathionylation of the sulfenic acid intermediate of 1-Cys-peroxiredoxin is important in the restoration of its function (32, 51).

While the importance of ERp57 and GSTP1 in posttranslational processing of reactive cysteines in proteins has clearly emerged, the client proteins interacting with these enzymes, their localization, and the mechanism of their action are still unknown. Thus, the goal of the current study was to determine whether Fas-SSG occurs during oxidative processing in the ER and whether this requires the action of ERp57. We also sought to explore the contribution of GSTP1 as a catalyst of Fas-SSG.

MATERIALS AND METHODS

Cell culture. Murine alveolar type II epithelial cells (C10) or primary lung fibroblasts from wild-type (WT) or *lpr* and *caspase3*$^{-/-}$ mutant mice and

Received 27 January 2012 Returned for modification 14 February 2012
Accepted 12 June 2012
Published ahead of print 2 July 2012
Address correspondence to Yvonne M. W. Janssen-Heininger, yvonne.janssen@uvm.edu.

doi:10.1128/MCB.00125-12

primary mouse tracheal epithelial cells (MTEC) were used. Cells were isolated and propagated as described elsewhere (3, 35, 41). Prior to treatment with FasL, C10 cells or fibroblasts were starved in serum-free, phenol red-free medium for 2 h. Cells were transfected with plasmids or short interfering RNA (siRNA) as described previously (3, 35).

Exposure of cells to FasL. C10 cells were treated with 150 ng/ml FLAG-FasL (Alexis, San Diego, CA) plus 0.5 μg/ml anti-FLAG cross-linking antibody (M2; Sigma, St. Louis, MO). Primary lung fibroblasts and MTECs were treated with 300 ng/ml FasL plus 1 μg/ml M2. As reagent controls, cells were treated with M2 alone.

IP of S-glutathionylated Fas. Immunoprecipitation (IP) of S-glutathionylated Fas was performed as described in reference 3.

Immunoprecipitation of Fas, ERp57, and GSTP1. C10 cells were treated with FasL and M2 for the indicated times. Lysates were prepared in buffer containing 20 mM Tris, pH 7.4, 150 mM NaCl, 10% glycerol, and 0.5% NP-40 with protease inhibitor cocktail. Five hundred micrograms of protein was used for immunoprecipitation using anti-Fas (JO2), anti-GSTP1, or ERp57 antibody (1 μg/ml) with protein G-agarose beads. The samples were analyzed by subsequent SDS-PAGE and probing of the Western blots. As a reagent control, lysates from cells exposed to FasL plus M2 for 1 h were incubated with isotype control IgG and subjected to the same procedures.

Cell viability assay. C10 cells or primary lung fibroblasts were plated in 12-well dishes. The MTT assay was performed as described previously (41). Results were obtained from 3 independent experiments conducted in triplicate.

Caspase-Glo assay. Caspase-8 and caspase-3 activities were measured using Caspase-Glo 8 and Caspase-Glo 3/7 (Promega, Madison, WI) reagents, respectively, according to the manufacturer's protocol (Promega, Madison, WI). Results were expressed in relative luminescence units (RLU) after subtraction of background luminescence values. All results were obtained from 3 independent experiments conducted in triplicate.

DISC isolation and analysis. DISC isolation was performed according to reference 20. Briefly, C10 cells (1×10^6 cells/60-mm dish) were transfected. Cells were starved for 2 h and then treated with FasL (1 μg/ml) plus the cross-linking antibody M2 (2 μg/ml) for 20 min at 37°C. Subsequent steps were performed on ice. Cells were washed once with phosphate-buffered saline (PBS) and lysed for 10 min in 500 μl of lysis buffer. All additional steps were performed as described in reference 3.

Cell fractionation. Cell fractionation was carried out using the Calbiochem ProteoExtractT (catalog no. 539790) subcellular proteome extraction kit per the manufacturer's protocol.

BLM model of fibrosis. C57BL/6J mice were instilled with bleomycin (BLM; 5.0 U/kg of body weight) oropharyngeally. Control (Ctr) siRNA (scrambled) or siRNA for ERp57 and GSTP1 (10 mg/kg; Thermo Scientific) was administered oropharyngeally 24 h prior to administration of bleomycin, as well as 5 and 10 days thereafter. Lungs were harvested on day 15 for histology, caspase activity, and Sircol collagen assays, as described previously (2). Masson's trichrome-stained lung sections were imaged using an Olympus BX50 light microscope with a QImaging Retiga 2000R digital camera. The images were captured at ×10 magnification. All studies were approved by the Institutional Animal Care and Use Committee at the University of Vermont.

Microscopy. Cells were fixed in 4% formalin and permeabilized with 0.2% Triton X-100 in PBS. Permeabilized cells were blocked in PBS containing 2% bovine serum albumin (BSA) for 1 h. Cells were sequentially incubated with primary antibodies (1:500; rabbit anti-ERp57 and mouse anti-Fas) and secondary antibodies (1:1,000; anti-rabbit Alexa Fluor 488-conjugated and anti-mouse Alexa Fluor 647-conjugated antibodies). The nucleus was stained with 4′,6-diamidino-2-phenylindole (DAPI) (1:4,000). Images were acquired using a Zeiss LSM 510 META confocal laser scanning imaging system. Images were captured at ×40 magnification in oil immersion. The image files were converted to Tiff format. Brightness and contrast were adjusted equally in all images.

Labeling of free sulfhydryls using MPB. Cells were lysed in HEPES buffer, pH 7.4, containing 0.5% NP-40 with 150 μM biotinylated *n*-ethyl maleimide (MPB) for 1 h at ambient temperature. Lysates were centrifuged at 14,000 rpm and passed through a Micro Bio-Spin (Bio-Rad) column to separate free MPB. The eluent whole-cell lysate was immunoprecipitated using an anti-Fas antibody and sequentially probed using streptavidin-horseradish peroxidase (HRP) and anti-Fas antibody.

Labeling of cell surface proteins using biotinylated DTSSP. Cells were treated with 0.5 mg of cell-impermeable biotinylated 3,3′-dithiobis sulfosuccinimidylpropionate (DTSSP) (Pierce) 30 min prior to harvest in Hanks balanced salt solution (HBSS) containing Ca^{2+} and Mg^{2+}. Cells were lysed in 20 mM Tris, pH 7.4, 150 mM NaCl, 10% glycerol, and 0.5% NP-40 with protease inhibitor cocktail. Lysates were centrifuged at 14,000 rpm and passed through a Micro Bio-Spin (Bio-Rad) column to separate free biotinylated DTSSP. The eluent whole-cell lysate was immunoprecipitated using an anti-Fas antibody and sequentially probed using streptavidin-HRP and anti-Fas antibody.

Antibodies. Antibodies against the following proteins/molecules were used in this study: rat anti-Fas (Upstate, Lake Placid, NY); rabbit anti-Fas (Santa Cruz); rabbit anti-GSTP1 and rat anti-FADD (MBL, Woburn, MA); rat anti-caspase-8 (Alexis, San Diego, CA); rabbit anticalreticulin and anti-caspase-3 (Cell Signaling, Danvers, MA); mouse anti-GSH (Virogen, Watertown, MA); streptavidin-conjugated HRP (Jackson, West Grove, PA); rabbit anti-Prx1, anti-Prx3, anti-Prx4, and anti-$PrxSO_3$ (Lab Frontier, Seoul, South Korea); goat ant-Grx1 (American Diagnostica, Stamford, CT); mouse anti-flotillin1 JO2 (BD Biosciences, San Jose, CA); rabbit and mouse anti-ERp57 and anti-PDI (Enzo Life Sciences, Plymouth Meeting, PA, and Abcam, Cambridge, MA); rabbit anti-ATF6 (Abcam, Cambridge, MA); and mouse anti-β-actin (Sigma, St. Louis, MO). The secondary HRP-conjugated anti-rabbit and anti-mouse antibodies were from Amersham (Piscataway, NJ). Anti-rat and anti-goat antibodies were from Jackson Laboratories (West Grove, PA). All of the fluorophore-conjugated antibodies were from Invitrogen (Carlsbad, CA).

Biochemical analysis of extra cellular GSH. Extracellular GSH was measured using an enzymatic recycling method (47) with few modifications. Proteins were precipitated from medium by adding 6.5% (wt/vol) sulfosalicylic acid (SSA). After 10 min, tubes were centrifuged for 15 min at 2,000 × *g*, and supernatants were stored at −80°C. Standards (0.5 to 100 nM GSH equivalent) were prepared by dilution in 10 mM HCl containing 1.3% SSA. 5,5′-dithiobis-2-nitrobenzoic acid (DTNB; 10 mM), NADPH (2 mM), and glutathione disulfide (GSSG) reductase (8.5 IU/ml) prepared in stock buffer containing 143 mM NaH_2PO_4, 6.3 mM EDTA, pH 7.4. The enzymatic reaction was started by addition of 40 μl/well of GSSG reductase and was monitored kinetically for 30 s to 2 min at a wavelength of 415 nm. The final concentrations of reagents were 0.73 mM DTNB, 0.24 mM NADPH, 0.09% SSA, and 1.2 IU/ml GSSG reductase.

PDI assay. Ten μg of total cell lysates was incubated with folded insulin, a fibril protein binding dye, for 1 h. The fluorescence was then measured in a microplate reader set with excitation at 500 nm and emission at 603 nm per the manufacturer's protocol (Proteostat protein disulfide isomerase [PDI] assay kit ENZ-51024-KP002). All results were obtained from 3 independent experiments conducted in triplicate.

GST activity assay. The GST activity was determined using a colorimetric activity assay kit (ab65326; Abcam, Cambridge, MA) and is based on the GST-catalyzed reaction between GSH and the GST substrate, CDNB (1-chloro-2,4-dinitrobenzene). The GST-catalyzed formation of CDNB-GSH produces a dinitrophenyl thioether which can be detected spectrophotometrically at 340 nm.

Synthesis of TLK199. *N*,*N*-Dimethylformamide and trifluoroacetic acid were purchased from Fisher Scientific (Pittsburgh, PA), 2-chlorotrityl chloride resin was from Novabiochem (San Diego, CA), and *O*-benzotriazole-*N*,*N*,*N*′,*N*′-tetramethyluronium hexafluorophosphate (HBTU) was from RS Synthesis (Louisville, KY). Fmoc-D-Phg-OH, Fmoc L-Cys(Bzl)-

OH, and Boc-Glu-OBut were purchased from Advanced Chemtech (Louisville, KY). TLK199 [γ-glutamyl-*S*-(benzyl)cysteinyl-*R*-phenyl glycine diethyl ester] was synthesized manually via Fmoc protocol on a 40 μmol scale using 2-chlorotrityl chloride resin (1.01 mmol/g). Double coupling of Fmoc amino acid derivatives using HBTU activation was employed for peptide elongation. A typical single coupling procedure is the following: 20% piperidine-DMF (2× for 10 min each), DMF washes (6× for 30 s each), 5 equivalents of Fmoc amino acid and HBTU in 0.4 M NMM-DMF (2× for 30 min each), and DMF washes (3× for 30 s). Cleavage of TLK199 from the resin was accomplished through treatment with 94:2:2:2 TFA-triisopropylsilane (TIPS)-H_2O-anisole for 2 h. Following filtration of the resin, the cleavage supernatant was evaporated to 1/10 its original volume in a stream of nitrogen, followed by precipitation of the crude peptide into cold anhydrous diethyl ether.

Image processing. Digital images were acquired by scanning X-ray film on a photo scanner (Perfection 5000; Epson). Photoshop (CS5; Adobe) and Illustrator (CS5; Adobe) were used to assemble the figures. Samples were run on the same gel. In some cases, lanes were assembled for consistency, as indicated by the vertical black line. When required, brightness and contrast were adjusted equally in all lanes.

Statistics. All assays were performed three times in triplicate (9 measurements). Data were analyzed by one-way analysis of variance (ANOVA) using the Bonferroni test to adjust for multiple comparisons or Student's *t* test where appropriate. Data from multiple experiments were averaged and are expressed as mean values ± standard errors of the means (SEM).

RESULTS

FasL causes rapid increases in S-glutathionylation of Fas (Fas-SSG) independently of overall changes in redox status or caspase activation. We previously showed that FasL-induced S-glutathionylation of Fas (Fas-SSG) was independent of activation of NADPH oxidases but was sustained by degradation of Grx1 (3). Protein S-glutathionylation is also dependent on alterations in GSH and glutathione disulfide (GSSG) ratios in the cell (51). Activation of the Fas pathway has been shown to cause GSH efflux from the cell, apparently increasing the levels of cytosolic GSSG (14). Following stimulation of cells with FasL in the presence of the cross-linking antibody M2, Fas-SSG was observed at 10 to 15 min and was sustained until 120 min (Fig. 1A), a time point at which we started to detect degradation of Grx1. The concentration of GSH in culture supernatants increased at 120 and 240 min after administration of FasL compared to the concentration of M2 control samples (Fig. 1B), but this did not occur at earlier time points. In contrast to the requirement of caspase-3 in contributing to increases in Fas-SSG 60 and 120 min following stimulation with FasL (3), results shown in Fig. 1C demonstrate that early increases in Fas-SSG formation observed at 15 or 30 min after stimulation with FasL occurred in cells lacking caspase-3. To determine whether the continuous presence of FasL is required for Fas-SSG, cells were incubated with FasL in the cold for 20 min. FasL was washed away or left in the cultures, and dishes were returned to 37°C. Results shown in Fig. 1D demonstrate that binding of FasL to surface Fas is sufficient to induce early but transient Fas-SSG, but it did not result in cleavage of caspase-3. Continuous FasL is required to induce sustained Fas-SSG and caspase-3 cleavage. Collectively, these data suggest that early increases in S-glutathionylation of Fas (Fas-SSG) occurred independently of changes in Grx1 content, caspase-3 activity, or efflux of GSH. We next examined whether FasL altered the redox status in specific subcellular compartments by monitoring overoxidation of Prx1, Prx3, or Prx4, which are localized in the cytosol, mitochondria, and endoplasmic reticulum (ER), respectively (21, 36, 44). Immunoprecipitation (IP) of Prx1, Prx3, or Prx4 and subsequent Western blotting for overoxidized forms of Prx ($PrxSO_3$) revealed rapid overoxidation of Prx4, which occurred within 10 min following ligation of Fas and was sustained for at least 120 min. In contrast, overoxidation of Prx1 and Prx3 also occurred in cells stimulated with FasL but at later time points compared to Prx4 (Fig. 1E). These findings suggest that FasL induces rapid alterations in the redox status of the ER. Despite these findings, FasL did not induce overt ER stress based on the absence of detection of the ER stress marker ATF6, in contrast to cells exposed to the ER stressor thapsigargin (THP) (Fig. 1F). We next sought to address the oxidative events that preceded Fas-SSG. Formation of a sulfenic acid (SOH) intermediate is well known as one of the potential oxidative events that can lead to protein S-glutathionylation. Cells were treated with the cell-permeable SOH trapping compound 5,5-dimethyl-1,3-cyclohexanedione (dimedone) (27, 39) prior to administration of FasL. Results shown in Fig. 1G demonstrate that formation of Fas-SSG was abolished in cells pretreated with dimedone, suggesting that Fas-SOH is required for the formation of Fas-SSG.

FasL induces oxidative processing of Fas and increases the interaction of ERp57 and GSTP with Fas. The extracellular/ligand binding domains of TNF receptors contain multiple cysteines that form intramolecular disulfide bridges (S-S) to create the ligand binding domain (7) that is essential for binding of the TNF family of ligands. Murine Fas contains 20 cysteines in its extracellular domain and 4 cysteines in the cytoplasmic death domain, one of which, Cys294, is the target for S-glutathionylation (3) (Fig. 2A). Based on the present findings which demonstrate increased oxidation of ER-localized Prx4, we investigated whether Fas is oxidatively folded following stimulation with FasL. Following exposure of cells to FasL, cells were lysed at different time points in the presence of MPB to label protein-free sulfhydryls. Fas was subsequently immunoprecipitated, and its free sulfhydryl content (SH) was assessed by probing Western blots with streptavidin-conjugated HRP. In control cells, robust labeling of Fas with MPB was observed, indicating the availability of Fas-SH groups in unstimulated cells. Within 5 min of FasL stimulation, MPB labeling was decreased, and by 10 to 30 min we failed to immunoprecipitate MPB-labeled Fas (Fig. 2B). The loss of Fas-SH groups indicated that pools of latent Fas undergo rapid oxidative processing following stimulation with FasL. It is possible that the loss of Fas-SH groups merely precedes S-glutathionylation of Fas at cysteine 294. To determine whether loss of Fas-SH groups is linked to S-glutathionylation of cysteine 294, Fas-deficient *lpr* mutant fibroblasts were transfected with wild-type Fas or C294A mutant, which cannot be S-glutathionylated (3). Results shown in Fig. 2C demonstrate a similar loss of Fas-SH content in cells expressing WT or C294A mutant Fas, indicating that the loss of SH labeling by MPB is not merely due to S-glutathionylation but likely is due to S-S bond formation of multiple cysteines in the extracellular domain.

Intramolecular disulfide (S-S) bond formation of protein cysteines is catalyzed by members of the family of protein disulfide isomerases (PDI) (22, 40, 5). Because of the rapid oxidation of Fas (Fig. 2B and C), we next investigated, by IP, whether Fas associates with any of the members of the PDI family. Results shown in Fig. 2D demonstrate a strong association of ERp57 with Fas upon stimulation with FasL. In contrast, under these conditions, no

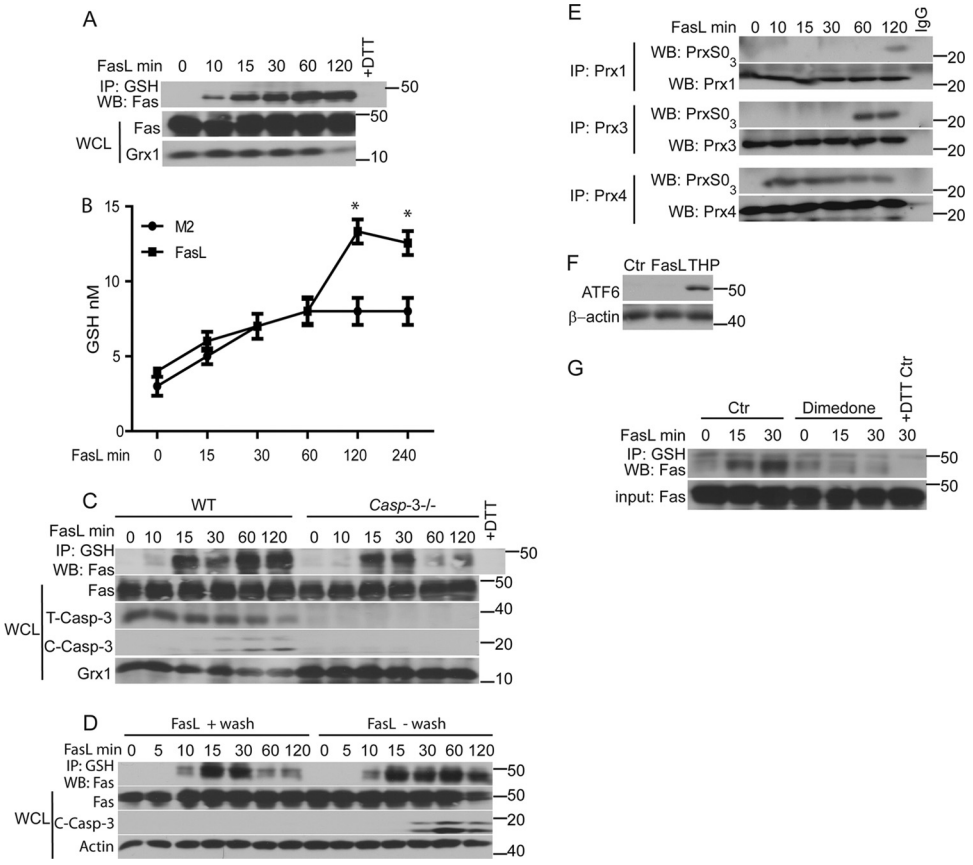

FIG 1 Early increases in Fas S-glutathionylation (Fas-SSG) occur independently of efflux of GSH or caspase activation and are associated with enhanced oxidation in the ER. (A) Rapid S-glutathionylation of Fas in response to FasL. C10 lung epithelial cells were stimulated with Flag-tagged FasL plus anti-Flag cross-linking antibody (M2) or M2 alone (0), and at the indicated times, lysates were prepared and immunoprecipitated (IP) using an anti-GSH antibody. The subsequent Western blot (WB) was probed with anti-Fas antibody (top). The +DTT control (Ctr) reflects lysates prepared from FasL-stimulated cells at 120 min and treated with 25 mM dithiothreitol (DTT) prior to IP with the anti-GSH antibody. Bottom panels show the content of Fas and Grx1 in whole-cell lysates (WCL). (B) FasL induces GSH efflux. C10 lung epithelial cells were stimulated with FasL plus M2 cross-linking antibody or M2 alone, and at the indicated times supernatants were collected. Free GSH was measured. *, $P < 0.05$ (by ANOVA) compared to M2 controls at the same time points. (C) Early formation of Fas-SSG does not require caspase-3. WT and *caspase3*$^{-/-}$ lung fibroblasts were treated with FasL as indicated. Lysates were subjected to IP with anti-GSH antibody, and subsequent Western blots were probed with Fas. Bottom panels show contents of Fas, total full-length caspase-3 (T-Casp-3), cleaved caspase-3 (active; C-Casp-3), and Grx1 in WCL. (D) Continuous presence of FasL is needed for sustained Fas-SSG and caspase-3 activation. C10 cells were treated with FasL in the cold for 20 min. FasL was washed away (+wash) or left in the dishes (−wash), and cells were then returned to 37°C for the indicated times. Lysates were processed as described for panel A. (E) Assessment of overoxidation of Prx in response to FasL. Prx1, Prx3, and Prx4 were immunoprecipitated following stimulation with FasL. Western blots were probed for overoxidized Prx ($PrxSO_3$) or with the respective immunoprecipitated Prx proteins as a control. (F) Stimulation of cells with FasL does not induce ER stress. C10 lung epithelial cells were stimulated with FasL plus M2, thapsigargin (THP), or M2 antibody/DMSO as a control (Ctr). Cells were lysed after 4 h. Western blots were probed for the ER stress marker, ATF6, and β-actin as a loading control. (G) A sulfenic acid intermediate (SOH) of Fas precedes its S-glutathionylation. Cells were incubated with the sulfenic acid-trapping agent, dimedone, for 2 h prior to stimulation of cells with FasL. Lysates were subjected to IP as described for panel A. Western blots were probed for Fas. The bottom panel shows input Fas in the WCL.

equivalent increase in interaction between PDI and Fas was observed.

Oxidation of SH groups to S-S by PDIs can generate H_2O_2 during their regeneration reaction via the ER-localized oxidoreductase Ero1 (17). Earlier experiments demonstrated that Fas-SSG is preceded by Fas-SOH (Fig. 1G), and it was previously demonstrated that SOH can be further S-glutathionylated by GSTP (32). Hence, we examined whether FasL stimulation increases the interaction of Fas with GSTP1. Indeed, Fas and GSTP1 coimmunoprecipitated, and their interaction was enhanced following FasL stimulation (Fig. 2E). Furthermore, the content of Fas on the cell surface and SDS-resistant, high-molecular-mass forms of ERp57 and Fas increased immediately after stimulation of cells with FasL (Fig. 2F and G). Collectively, these results demonstrate that rapid oxidation of Fas occurs upon stimulation of cells with FasL, which correlated with associations between the disulfide-forming enzyme, ERp57, and Fas and between the S-glutathionylating enzyme, GSTP1, and Fas.

Epithelial cells have been shown to undergo apoptosis via a mitochondrion-dependent amplification pathway, whereas fibroblasts undergo apoptosis independently of mitochondria (10, 34). Indeed, results shown in Fig. 2H demonstrate higher increases in mitochondrion-dependent caspase-9 activity in response to FasL in epithelial cells than in fibroblasts, while activities of caspase-3 and -8 were comparable in both cell types. The purity of these primary cell cultures was confirmed by Western blotting for

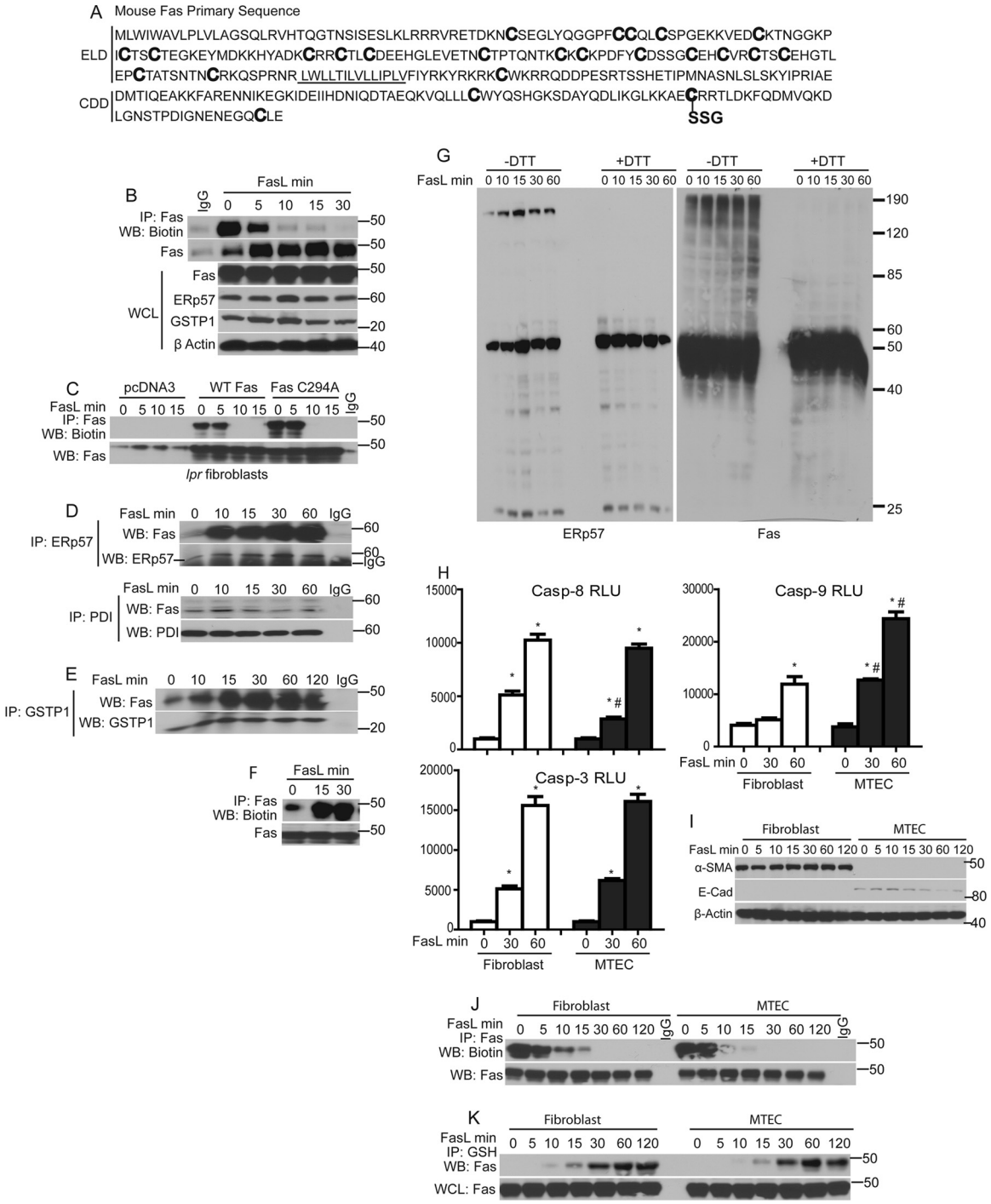

FIG 2 FasL induces oxidative processing of latent Fas and a rapid interaction between ERp57, GSTP1, and Fas. (A) Primary sequence of murine Fas (NP_032013; www.ncbi.nlm.nih.gov/protein/NP_032013.2), showing cysteines (boldface) in the ligand binding domain predicted to form disulfide bridges, and the death domain cysteines, including Cys294, which is S-glutathionylated (SSG). The transmembrane domain is underlined. ELD, extracellular ligand binding domain; CDD, cytoplasmic death domain. (B) FasL induces rapid oxidative processing of latent Fas. C10 lung epithelial cells were treated with FasL. Lysates were labeled with MPB and subjected to IP using an anti-Fas antibody. Western blots were probed sequentially with streptavidin-conjugated HRP and anti-Fas antibody (top panels). The bottom gels are WCL showing contents of Fas, ERp57, GSTP1, and β-actin. (C) FasL induces rapid oxidative processing of wild-type Fas or Cys294A mutant Fas. WT and *lpr* mutant mouse lung fibroblasts were treated with FasL. Lysates were processed as described for panel B. (D) FasL induces rapid association of latent Fas with ERp57. Cells were treated with FasL as indicated, and lysates were subjected to IP using anti-ERp57 and anti-PDI antibodies or preimmune IgG as a control. Western blots were probed sequentially with anti-Fas and anti-ERp57 (top) or anti-Fas and anti-PDI (bottom) antibodies. (E) FasL induces a rapid association of Fas with GSTP1. Cells were treated with FasL, and lysates were subjected to IP using anti-GSTP1 antibody or control IgG. Blots were probed sequentially with anti-Fas and GSTP1 antibodies. (F) FasL increases membrane Fas localization. C10 cells were stimulated with FasL for the indicated times. Prior to harvest, cells were incubated with biotinylated DTSSP, and lysates were subjected to IP with anti-Fas antibody. Blots were probed sequentially with streptavidin-conjugated HRP and anti-Fas antibody. (G) FasL induces DTT-sensitive high-molecular-mass forms of ERp57 and Fas. Cells were treated with FasL and

α-smooth muscle actin (fibroblasts) and E-cadherin (epithelial cells) (Fig. 2I). Oxidative processing and Fas-SSG were similar in fibroblasts or epithelial cells in response to FasL (Fig. 2J and K), suggesting that Fas oxidations occurred irrespective of an involvement of mitochondria in apoptosis.

Interaction of ERp57 and GSTP1 with Fas and S-glutathionylation of Fas in the ER. ERp57 is a PDI that resides in the ER (11). The presence of Fas and GSTP1 in the ER has not been documented. Hence, we next sought to explore the subcellular compartment in which ERp57, GSTP, and Fas interact, and whether this coincides with Fas-SSG. For this purpose, cells were fractionated into cytosol/plasma membrane (pm), ER, and nuclear fractions, as identified by the markers Prx1/flotillin1, calreticulin (CRT), and histone H3, respectively. As expected, in control cells, ERp57 was found only in fraction 2, which also contained the ER marker protein, CRT (Fig. 3A). Fas was readily detectable in the ER (fraction 2), as well as nucleus (fraction 3) and, to some extent, in cytosol/pm (fraction 1). GSTP1 was found in both cytosol/pm and ER fractions, although it was predominantly in the cytosol/pm. Within 15 min of stimulation of cells with FasL, the Fas content in the cytosol/pm increased (Fig. 3A). The S-glutathionylated form of Fas was first detected in the ER by 10 min and started to appear in cytosol/pm at 15 min, and it was sustained for at least 30 min after FasL stimulation (Fig. 3A, top lanes). We next evaluated the subcellular interaction of Fas with ERp57 using confocal laser scanning microscopy. Results shown in Fig. 3B demonstrate that in control cells, no colocalization of Fas and ERp57 was detected. However, increased colocalization of Fas and ERp57 was apparent within 10 min after stimulation with FasL, with further increases apparent by 30 min after stimulation. IP of GSTP1 from fractions 1 and 2 indicated some association between Fas and GSTP in the ER in control cells and increased associations upon stimulation with FasL, which were predominantly in the ER by 10 min. However, 15 and 30 min after FasL stimulation, interactions of Fas and GSTP1 increased in both ER and cytosolic/pm fractions (Fig. 3C). We next sought to characterize whether the movement of Fas-SSG from ER to cytosol/pm is dependent on anterograde transport using an anterograde transport blocking agent, brefeldin A (26). In brefeldin A-treated cells stimulated with FasL, Fas-SSG remained restricted to the ER fraction, and no Fas was detected in the cytosol/pm, in contrast to cells treated with dimethylsulfoxide (DMSO) vehicle control (Fig. 3D). In aggregate, these results demonstrate that in response to ligation of surface Fas, oxidative processing and S-glutathionylation of a separate pool of Fas occurs in the ER, in association with increased interactions between Fas, ERp57, and GSTP1.

Knockdown of ERp57 and GSTP1 decreases oxidative processing and S-glutathionylation of Fas and increases cell survival. To address the functional importance of ERp57 and GSTP in oxidative processing, S-glutathionylation of Fas, and ramifications for apoptosis, ERp57 and GSTP1 were ablated individually or simultaneously in epithelial cells. Results shown in Fig. 4A demonstrate an almost complete loss of Fas-SSG in cells lacking ERp57 upon ligation of Fas compared to siRNA controls (top). Smaller but consistent decreases in FasL-stimulated Fas-SSG were also observed following siRNA-mediated knockdown of GSTP1. Simultaneous ablation of both ERp57 and GSTP1 resulted in a complete loss of detectable Fas-SSG in response to FasL (Fig. 4A, bottom), demonstrating that the coordinate action of ERp57 and GSTP1 is required for FasL-induced Fas-SSG. Previous experiments demonstrated a rapid FasL-induced loss of sulfhydryl content of Fas (Fas-SH) (Fig. 2B). Since we observed a complete loss of Fas-SSG following siRNA-mediated ablation of ERp57 and GSTP1 siRNA samples, we assessed Fas-SH in cells lacking ERp57 and GSTP1 following stimulation with FasL. Consistent with results shown in Fig. 2B, a rapid loss of Fas-SH occurred in response to FasL in control siRNA-transfected cells (Fig. 4B). In contrast, following knockdown of both ERp57 and GSTP1, Fas-SH content was equivalent to that of unstimulated cells up to 15 min after stimulation with FasL, although some decreases in sulfhydryl content were apparent at later time points (Fig. 4B). We next tested whether the decreases in oxidative processing and S-glutathionylation of Fas in cells lacking ERp57 and GSTP had any effect on death-inducing signaling complex (DISC) formation. Cells were exposed to the FasL-oligomerizing antibody (M2) alone or to FasL plus M2. As expected, IP of the DISC demonstrated associations between Fas, FADD, and caspase-8 following incubation of cells with FasL but not with M2 alone. Interestingly, both ERp57 and GSTP also coimmunoprecipitated with the DISC in FasL-treated cells. In cells with decreased levels of ERp57 and GSTP1, functional DISC assembly did not occur following Fas ligation, based upon the absence of Fas, FADD, and procaspase-8 that coimmunoprecipitated with FasL, compared to control siRNA (Fig. 4C). siRNA-based ablation of ERp57 or GSTP1 resulted in decreased activities of caspase-3 and -8 and diminished cell death in response to FasL compared to control siRNA (Fig. 4D to F). Simultaneous knockdown of ERp57 and GSTP1 resulted in further decreases in caspase-3 and -8 activities upon Fas ligation and further rescued cells from FasL-induced death compared to the knockdown of proteins individually (Fig. 4D to F).

Pharmacologic inhibition of ERp57 and GSTP1 decreases Fas-SSG and caspase activation. We next assessed the contribution of the catalytic activities of ERp57 and GSTP in mediating S-glutathionylation of Fas and subsequent activation of caspases. We incubated epithelial cells with thiomuscimol, a known inhibitor of PDIs (19), or its inactive analog, muscimol, for 2 h at 37°C. Thiomuscimol-treated cells showed an ~50% decrease in insulin-reducing activity compared to the muscimol controls (Fig. 5A). Validation of the insulin-reducing assay using ERp57 siRNA demonstrated an ~45% decrease in insulin-reducing activity compared to control siRNA-transfected cells, indicating that a substantial amount thiomuscimol-inhibitable insulin-reducing activity is due to ERp57 (Fig. 5B). Thiomuscimol significantly attenuated Fas-SSG in response to FasL compared to muscimol controls (Fig. 5C), with corresponding decreases in activities of caspase-3 and -8 (Fig. 5D and E).

lysates subjected to nonreducing (−DTT) and reducing (+DTT) SDS-PAGE. Blots were probed with ERp57 or Fas antibodies. Approximate molecular sizes (in kDa) are indicated. (H) Measurement of caspase activities in primary lung fibroblasts and tracheal epithelial cells (MTEC) following stimulation with FasL. (I) Confirmation of purity of primary fibroblasts and MTEC via Western blotting for the epithelial marker E-cadherin (E-cad) or the fibroblast marker α-smooth muscle actin (α-SMA). Assessment of oxidative processing (J) and S-glutathionylation of Fas (K) in fibroblasts and epithelial cells stimulated with FasL is also shown. Lysates were labeled and processed as described for panel B and Fig. 1A, respectively.

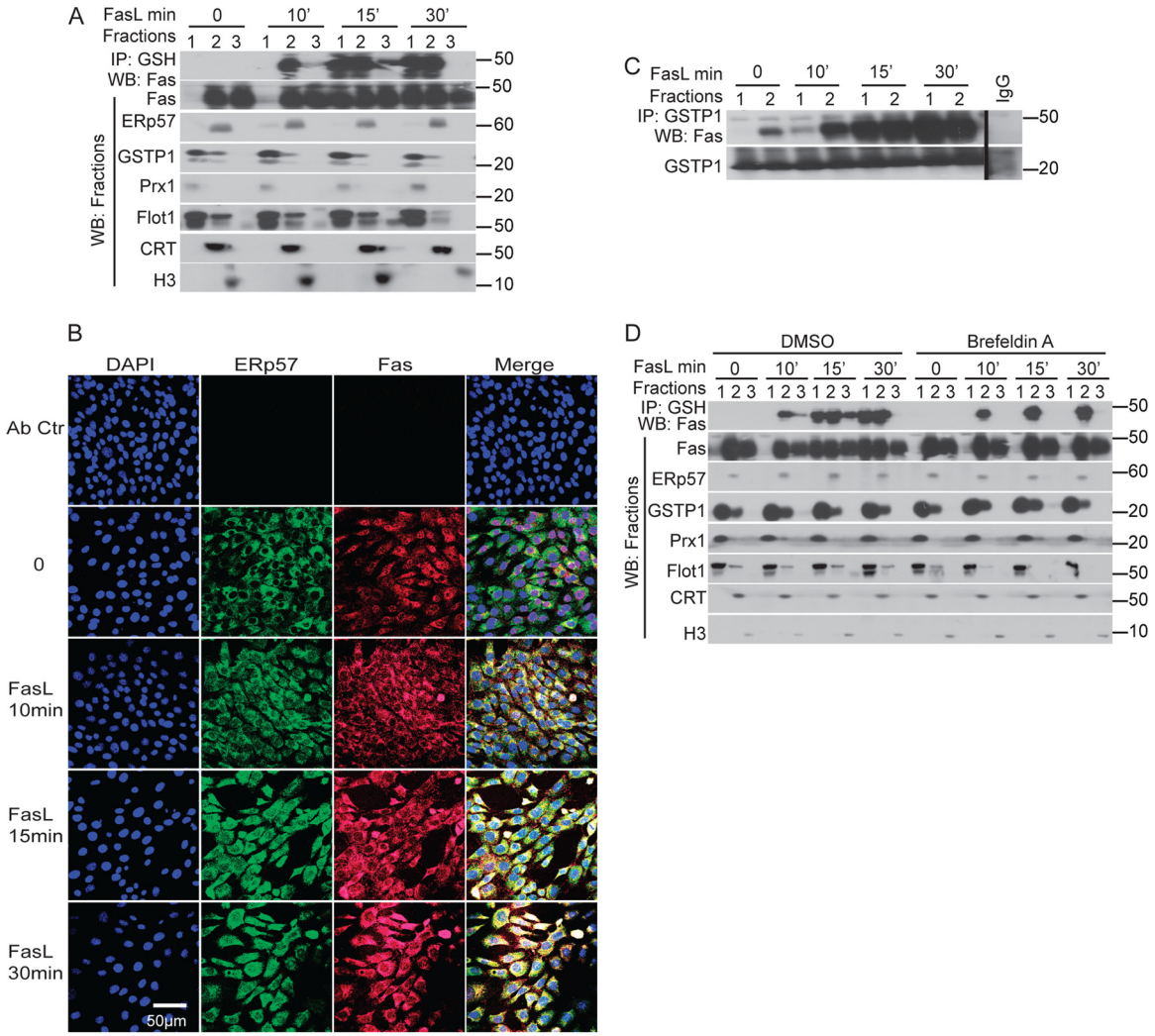

FIG 3 Localization of ERp57, Fas, and GSTP1 and S-glutathionylation of Fas in the ER. (A) C10 cells were stimulated with FasL, and cells were fractionated into cytosolic/plasma membrane (lanes 1), endoplasmic reticulum (lanes 2), and nucleus (lanes 3). Proteins from each fraction were subjected to IP using anti-GSH antibody (Ab). Western blots were probed for Fas. Twenty-five μg of total protein from each fraction was separated on an SDS-PAGE and probed for Fas, ERp57, GSTP1, Prx1 (cytosolic protein), flotillin1 (Flot1; plasma membrane protein), calreticulin (CRT; an ER restricted protein), and histone H3 (nuclear marker). (B) Fas colocalizes with the ER protein ERp57. Cells were treated with FasL and stained with ERp57 (green), Fas (red), and the nuclear marker DAPI (blue). Yellow staining in merged images indicates colocalization of Fas and ERp57. (C) Stimulation with FasL causes an enhanced interaction between GSTP1 and Fas. Proteins from fractions characterized in panel A were subjected to IP using anti-GSTP1 antibodies or control IgG. (D) Fas is S-glutathionylated in the ER and then translocated to the cytosol/PM fraction. Epithelial cells were treated with FasL in the presence or absence of brefeldin A. Cells were fractionated as described for panel A, and proteins from each fraction were subjected to IP using anti-GSH antibody. Western blots were probed for Fas. Twenty-five μg of total protein from each fraction was separated by SDS-PAGE and probed for Fas, ERp57, GSTP1, Prx1 (cytosol), Flot1 (plasma membrane), CRT (ER), and H3 (nucleus).

TLK199 is a highly specific inhibitor of GSTP (31). Results shown in Fig. 5F demonstrate that incubation of cells with 50 μM TLK199 resulted in an 80% decrease in GSTP activity. FasL-mediated increases in Fas-SSG, caspase-3, and caspase-8 activities were all diminished in cells exposed to TLK199 (Fig. 5G to I). Collectively, these results demonstrate that the coordinated catalytic activities of ERp57 and GSTP contribute to Fas-SSG and subsequent activation of caspases.

In addition to Fas, the extracellular/ligand binding domains of other members of the TNF receptor superfamily also contain cysteines that form intramolecular disulfide bridges (S-S) to create the ligand binding domain (7). We therefore determined whether ERp57-mediated oxidative processing regulates TNFR-dependent apoptosis. Cells were incubated with the ERp57 inhibitor, thiomuscimol, prior to stimulation with TNF-α in the presence of cycloheximide (CHX) to induce apoptosis. Results shown in Fig. 5J demonstrate that TNF-α/CHX-mediated activation of caspase-3 was significantly decreased by thiomuscimol, while the muscimol control did not affect apoptosis. These findings suggest that ER-dependent oxidative processing also affects apoptosis induced via other members of the TNFR superfamily, although additional analyses are required to strengthen this possibility.

Overexpression of Prx4 decreases S-glutathionylation of Fas, caspase activation, and cell death. Based on our findings demon-

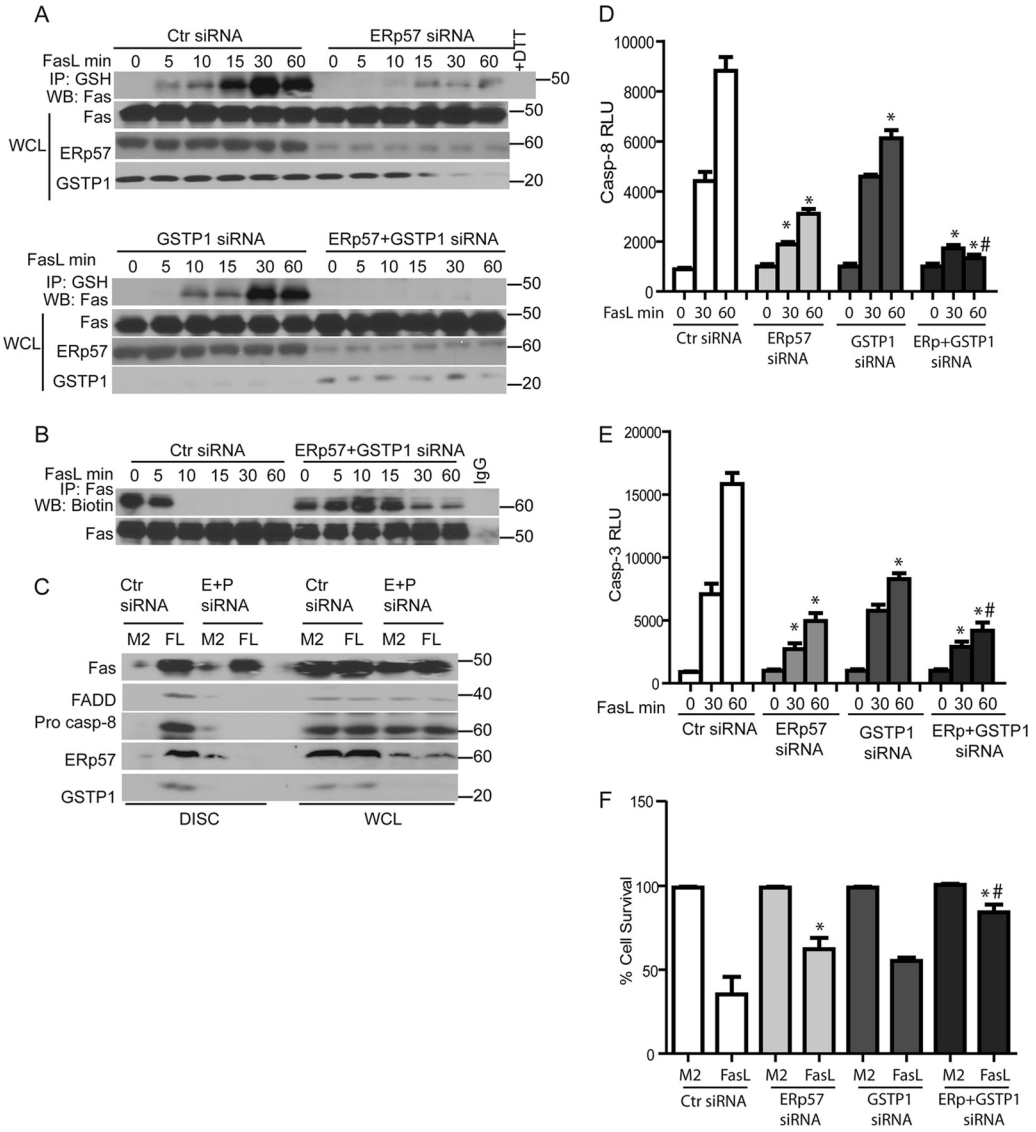

FIG 4 Knockdown of ERp57 and GSTP1 decreases FasL-induced S-glutathionylation of Fas and increases cell survival. (A) Cells were transfected with control (Ctr), ERp57 (top), GSTP1, or ERp57 and GSTP1 (bottom) siRNAs. Cells were exposed to FasL, and cell lysates were processed as described in the legend to Fig. 1A. Western blots from WCL were sequentially probed for Fas, ERp57, and GSTP1. (B) FasL-induced oxidative processing of Fas was attenuated in cells lacking ERp57 and GSTP1. Cells were treated with FasL, and lysates were processed as described in the legend to Fig. 2B. (C) FasL-induced formation of the death-inducing signaling complex (DISC) is attenuated in cells lacking ERp57 and GSTP1. Cells were transfected with ERp57 and GSTP1 siRNA (E+P), and 24 h later they were exposed to FasL+M2 cross-linking antibody (FL) or M2 alone for 30 min. Cell lysates were subjected to IP of the DISC. Western blots were sequentially probed for Fas, FADD, procaspase-8, ERp57, and GSTP1. WCL indicates the assessment of the same proteins in whole-cell lysates as a control. Knockdown of ERp57 and GSTP1 decreases caspase-8 (D) and caspase-3 activity (E) and increases cell survival (F) according to MTT assay 4 h following stimulation with FasL. *, $P < 0.05$ by ANOVA compared to Ctr siRNA groups. #, $P < 0.05$ compared to ERp57 or GSTP1 siRNA groups.

strating that FasL led to increased oxidation of ER-localized Prx4 and subsequent Fas-SSG, we speculated that overexpression of Prx4 quenches the H_2O_2 produced in response to oxidative folding and decreases Fas-SSG. As expected, overexpression of Prx4 resulted in higher levels of Prx4 overoxidation, reflective of quenching of H_2O_2 (Fig. 6A). Overexpression of Prx4 did not inhibit FasL-mediated oxidative folding of Fas (Fig. 6B) but almost completely prevented subsequent Fas-SSG (Fig. 6C). Furthermore, overexpression of Prx4 also resulted in significantly decreased caspase-3 and -8 activities and increased cell survival in response to FasL (Fig. 6D to F). These findings suggest that Prx4 acts downstream of the oxidative folding of Fas, and that H_2O_2 produced during oxidative folding is required for subsequent formation of Fas-SSG.

Calcium chelation abolishes oxidative folding and decreases Fas-SSG, caspase activation, and apoptosis. Calcium (Ca^{2+}) has been shown to play a critical role in Fas-mediated apoptosis (50). To determine whether oxidative processing of Fas is dependent on calcium, cells were incubated with a cell-permeable Ca^{2+} chelator, BAPTA-AM (Tocris). Results shown in Fig. 7A and B demonstrate that preincubation of cells with BAPTA-AM completely prevented the loss of Fas-SH groups observed in response to FasL and

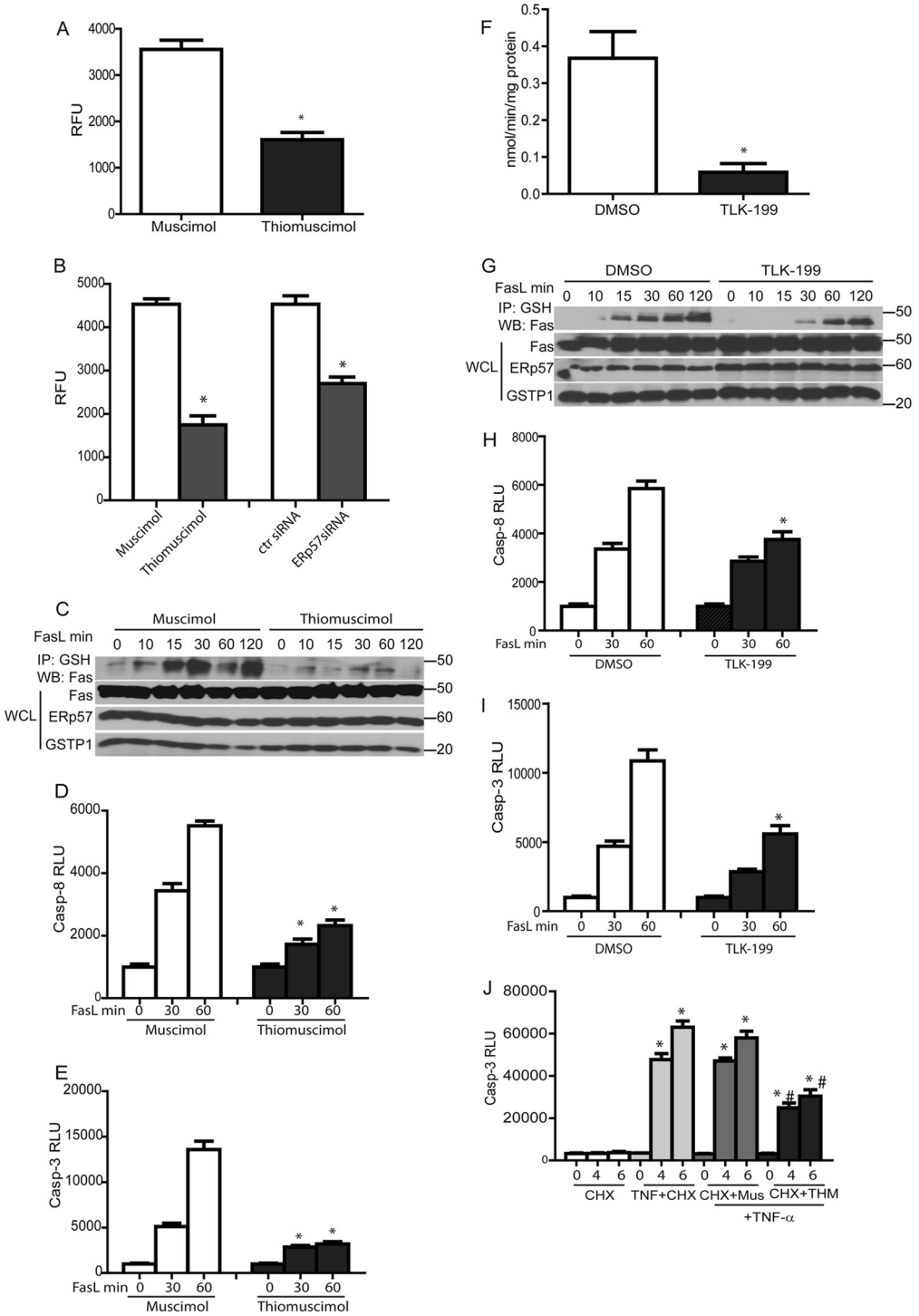

FIG 5 Inhibition of ERp57 and GSTP1 decreases FasL-induced S-glutathionylation of Fas and caspase activity. (A) Cells were incubated with the PDI inhibitor, thiomuscimol (10 μM), or its inactive analog, muscimol (10 μM), for 1 h prior to determination of PDI activity using an insulin reduction assay. Results are expressed as relative fluorescence units (RFU). *, $P < 0.05$ (Student *t* test) compared to muscimol-treated cells. (B) Determination of PDI activity (as described in the legend to panel A) in thiomuscimol- and ERp57 siRNA-treated cells. *, $P < 0.05$ (by Student *t* test) compared to control cells. (C) Cells were preincubated with the PDI inhibitor, thiomuscimol (10 μM), or its inactive analog, muscimol (10 μM), for 1 h prior to stimulation with FasL for the indicated times. Cell lysates were processed as described in the legend to Fig. 1A to determine the level of Fas-SSG. (D and E) Inhibition of ERp57 decreases caspase-3 and caspase-8 activities. *, $P < 0.05$ by ANOVA compared to muscimol-treated cells. (F) Cells were incubated with GSTP inhibitor, TLK-199 (50 μM), or 0.2% DMSO for 2 h prior to determination of the GSTP activity using the CDNB-GST assay. Results are expressed as nmol of CDNB oxidized/min/mg protein. *, $P < 0.05$ (by Student *t* test) compared to DMSO controls. (G) TLK199 decreases Fas-SSG. Cells were preincubated with TLK-199 or DMSO for 2 h prior to stimulation with FasL. Lysates were processed as described in the legend to Fig. 1A. Inhibition of GSTP decreases the activities of caspase-8 (H) and -3 (I) induced by FasL. *, $P < 0.05$ by ANOVA compared to DMSO controls. (J) Effect of thiomuscimol on TNF-α plus cycloheximide (CHX) induced caspase-3 activation. Mus, muscimol control. *, $P < 0.05$ by ANOVA compared to TNF-α+CHX controls.

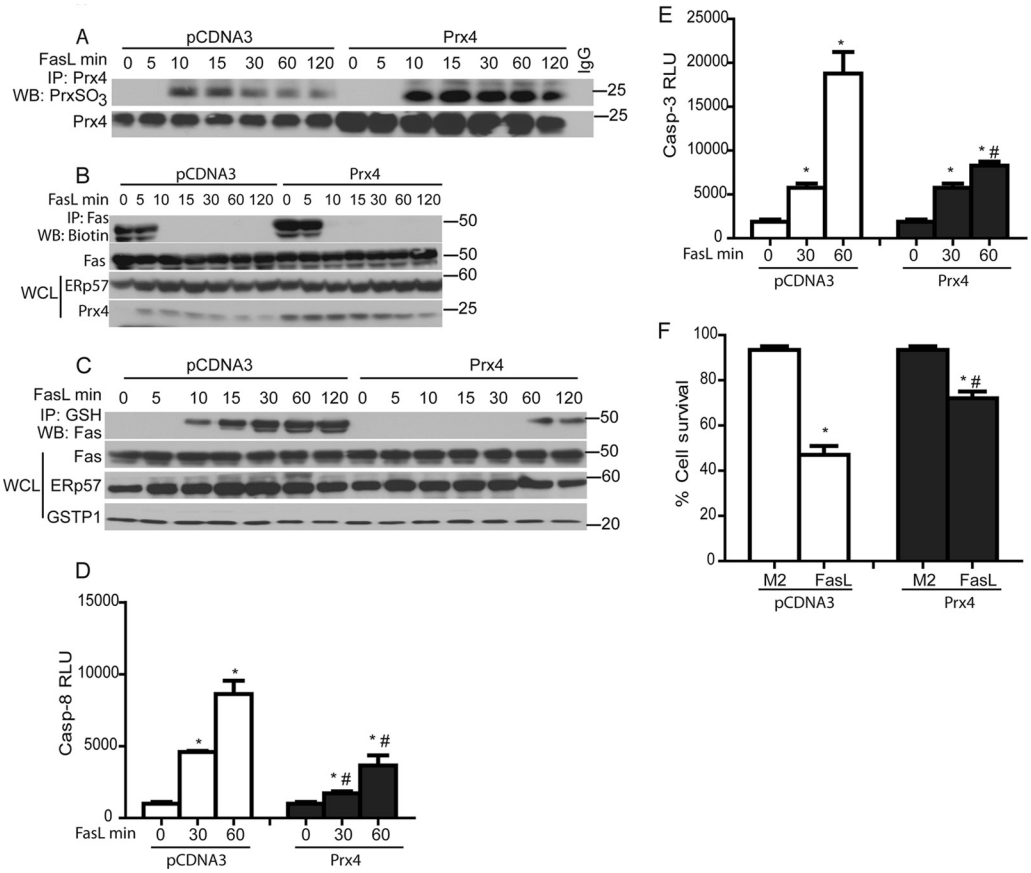

FIG 6 Prx4 does not affect Fas-SH but decreases FasL-induced Fas-SSG and apoptosis. (A) Assessment of overoxidation of Prx4 (top) following its overexpression (bottom). (B) Lack of impact of Prx4 overexpression on oxidative processing of Fas. Cells were transfected with pCDNA3 and Prx4 plasmids and subsequently treated with FasL. The lysates were processed as described in the legend to Fig. 2B. The bottom panel shows Prx4 and ERp57 content in WCL. Prx4 overexpression decreases Fas-SSG (C), caspase-3 and -8 activities (D and E), and cell death (F) in response to FasL. *, $P < 0.05$ by ANOVA compared to M2 controls. #, $P < 0.05$ compared to pCDNA3.

substantially diminished Fas-SSG. Furthermore, chelation of Ca^{2+} resulted in decreased caspase-3 and -8 activities and increased cell survival in response to FasL (Fig. 7C to E). These findings suggest that a Ca^{2+}-dependent signal is required for the induction of oxidative processing and S-glutathionylation of latent Fas in the ER.

Overexpression of ERp57 and GSTP enhances S-glutathionylation of Fas, caspase activity, and cell death. To determine the effect of overexpression of ERp57 or GSTP1 in FasL-induced cell death, cells were transfected with pcDNA3, GSTP1, or ERp57 cDNAs. Fractionation of cells overexpressing both ERp57 and GSTP1 demonstrated that by 10 min of FasL stimulation, Fas-SSG and total Fas content were already increased in the cytosol/pm fraction (fraction 1), in contrast to pcDNA3-transfected cells, where Fas-SSG remained restricted to the ER (fraction 2) and Fas was largely absent from the cytosol/pm (Fig. 8A). Overexpression of ERp57 or GSTP1 individually resulted in small increases in FasL-induced activation of caspase-3 and -8, as well as cell death, compared to pcDNA3-transfected cells. However, overexpression of both ERp57 and GSTP1 simultaneously led to further increases in FasL-induced activities of caspase-3 and -8 and resulted in enhanced cell death compared to individual control groups (Fig. 8B to D). In aggregate, these findings demonstrate that ERp57 and GSTP1 enhance the kinetics of Fas-SSG and movement of Fas into the membrane/cytosol, and they cooperate to enhance caspase activation and cell death.

Knockdown of ERp57 and GSTP1 inhibits bleomycin-induced pulmonary fibrosis in mice. We finally sought to corroborate the functional relevance of these observations in the bleomycin model of acute lung injury and fibrosis, which has been shown to require functional Fas (16, 28, 49). C57BL/6 mice were instilled oropharyngeally with siRNA for ERp57 and GSTP1 (E+G siRNAs) 1 day prior to administration of BLM and 5 and 10 days thereafter. Results shown in Fig. 9A and B demonstrate that increases in collagen content in lung tissue and histopathology 15 days after administration of bleomycin were significantly attenuated in mice receiving ERp57 and GSTP1 siRNAs compared to scrambled siRNA-instilled mice. Similarly, increases in caspase-3 and -8 activities following instillation of bleomycin were also significantly inhibited in mice following knockdown of ERp57 and GSTP1 compared to Ctr siRNA-instilled mice (Fig. 9C and D).

We next sought to determine whether bleomycin-induced Fas-SSG was decreased in mice lacking ERp57 and GSTP1. Results shown in Fig. 9E demonstrate robust increases in Fas-SSG in mice instilled with Ctr siRNA 15 days following administration of BLM,

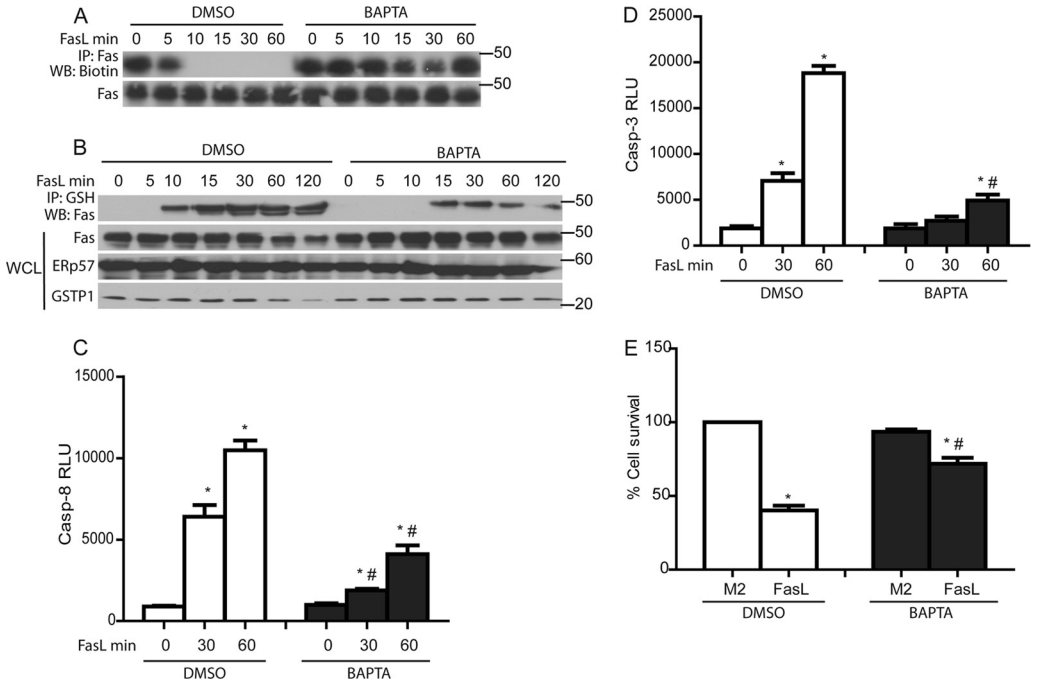

FIG 7 Chelation of Ca^{2+} decreases FasL-induced oxidative processing of Fas and Fas-SSG as well as epithelial cell apoptosis. BAPTA inhibits oxidative processing of Fas (A) and decreases Fas-SSG (B), caspase-3 and -8 activities (C and D), and cell death (E) in response to FasL. *, $P < 0.05$ by ANOVA compared to M2 controls. #, $P < 0.05$ compared to DMSO-treated cells.

while very little Fas-SSG was detected in mice following knockdown of ERp57 and GSTP1. Immunoprecipitation of Fas from lung tissues of BLM-treated animals showed strong interactions with ERp57 and GSTP1, which were not detected in the PBS control group. As expected, the overall content of ERp57 and GSTP in lung tissue and their interaction with Fas was decreased in response to their siRNA-mediated ablation (Fig. 9E and F). Taken together, these results illuminate the potential pathophysiological relevance of ERp57- and GSTP-mediated S-glutathionylation of Fas in fibrotic disease in which a causal role of Fas has been suggested (49).

DISCUSSION

The regulation of biological processes by redox-active enzymes is becoming increasingly appreciated, and regulatory roles for dynamic cysteine oxidations, such as disulfide (S-S) and mixed disulfide (S-SG) bonds, are emerging. However, the relevance of these events, precise molecular targets, and the redox-active enzymes involved in apoptotic signaling are still obscure. Our earlier investigation into the involvement of a redox-based mechanism in Fas-dependent apoptosis demonstrated that initial ligation of Fas triggers subsequent S-glutathionylation of Fas (Fas-SSG) at Cys294, which is sustained by caspase-dependent degradation of the deglutathionylating enzyme, Grx1. We also previously unraveled that Fas-SSG enhances DISC assembly, promotes further activation of caspases, and represents a regulatory mechanism to amplify apoptosis (3). However, the biochemical events that are responsible for the S-glutathionylation of Fas remained unknown. Results from the present study demonstrate that Fas-SSG occurred rapidly, prior to overall changes in the cellular redox state, measured by efflux of GSH and overoxidation of Prx1 and Prx3. We also demonstrate here that early increases in Fas-SSG were independent of caspase-3 and occurred prior to degradation of Grx1. Instead, we demonstrate here that S-glutathionylation of Fas is catalyzed by coordinated actions of two enzymes, i.e., ERp57 and GSTP1 (Fig. 9G). The present study illuminates that distinct pools of Fas exist, including a latent pool, which is not oxidatively processed into the mature form capable of ligand binding. Following stimulation with FasL, latent Fas is processed by ERp57 in the ER. During oxidative processing of Fas in the ER, H_2O_2 is produced, which in turn facilitates S-glutathionylation of Cys294 via a GSTP-dependent mechanism. These findings illuminate a new dimension to our knowledge of Fas-induced apoptosis and suggest a regulatory switch, the ligand-initiated oxidative processing of latent Fas, to control the strength of the apoptotic signal. These results also demonstrate that highly compartmentalized changes in the cellular redox environment mediate S-glutathionylation of Fas.

The signaling events that initiate oxidative processing of Fas in the ER upon stimulation of cells with FasL remain unknown. Given the rapid loss of free thiol content of Fas that is already apparent after 5 min, these events are induced rapidly and are unlikely to require internalization of Fas (12) or assembly of the DISC (Fig. 4C). Previous work showed that FasL-induced increases in phospholipase C-γ1 (PLC-γ1) activity mediate rapid release of Ca^{2+} via inositol 1,4,5-triphosphate receptor (IP_3R) channels, which were required for Fas-mediated apoptosis (50). Results from the present study not only confirm the role of Ca^{2+} in Fas-mediated apoptosis but also demonstrate a putative role for Ca^{2+} in mediating rapid ERp57-dependent oxidative processing in the ER. Further studies will be necessary to formally address the precise mechanisms by which Ca^{2+} regulates FasL-induced, ERp57-dependent rapid oxidative processing of Fas and apoptosis.

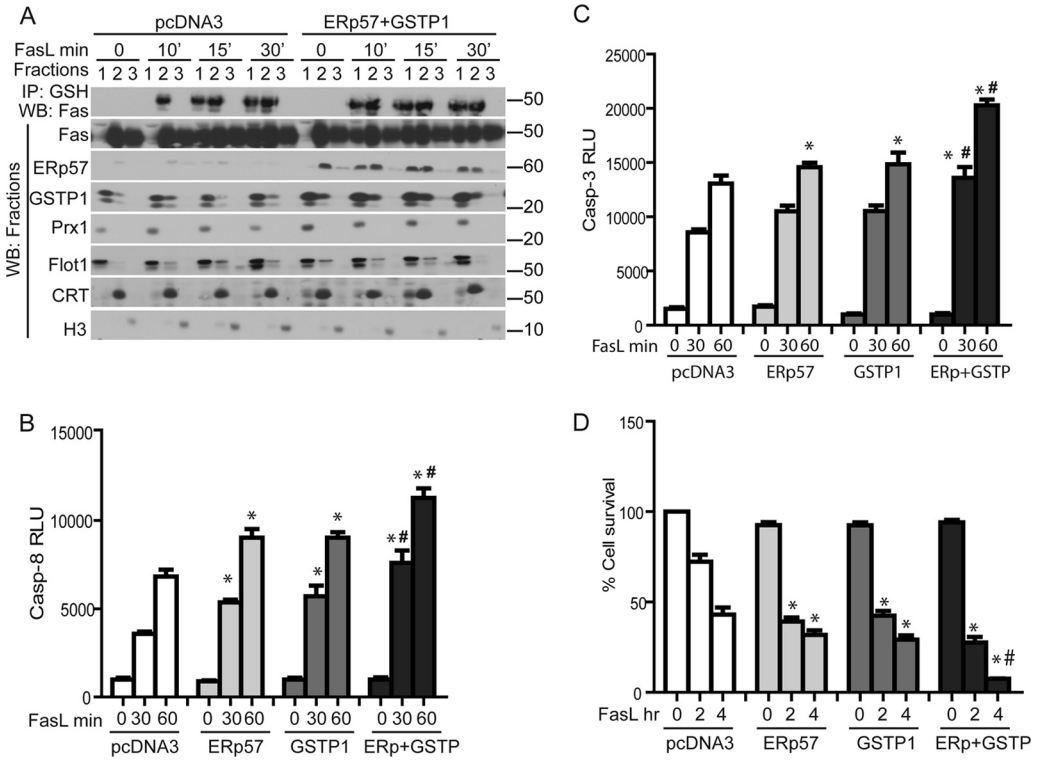

FIG 8 Overexpression of ERp57 and GSTP1 increases the kinetics of translocation of S-glutathionylated Fas from the ER to the cytosolic/plasma membrane fraction and decreases cell survival in response to FasL. (A) Assessment of Fas-SSG in cytosol/plasma membrane fractions (fraction 1), ER (fraction 2), and nucleus (fraction 3) in cells overexpressing ERp57 and GSTP. C10 lung epithelial cells were transfected with pCDNA3 or pERp57 plus pGSTP1 plasmids for 24 h prior to exposure to FasL. Cell fractionations were prepared for IP using anti-GSH antibody and for WB as described in the legend to Fig. 3A. Overexpression of ERp57 and GSTP1 increases caspase-8 (B) and caspase-3 (C) activities and cell death (D). *, $P < 0.05$ compared to pcDNA3 control groups. #, $P < 0.05$ compared to cells transfected with ERp57 or GSTP1 individually (ANOVA).

The extracellular ligand binding domain of Fas consists of 20 cysteines, which are predicted to be in the form of 10 intramolecular disulfide bridges (S-S) (8). We demonstrate here that ERp57 plays a cardinal role in the oxidative folding of Fas, ultimately leading to S-glutathionylation of Cys294. The exact stoichiometry and regulatory events that govern ERp57-catalyzed disulfide bond formation, sulfenic acid formation, and S-glutathionylation of Fas require further analyses. The loss of free sulfhydryl content of Fas in cells expressing Cys294Ala mutant Fas, which cannot be S-glutathionylated (Fig. 2C) (3), and the preferential effect of overexpression of Prx4 on attenuating Fas-SSG but not the loss of Fas-SH following FasL (Fig. 6B and C), suggest that oxidative processing of Fas by ERp57 and S-glutathionylation are separate events. We speculate that increases in H_2O_2 formed during regeneration of oxidized ERp57 causes a sulfenic acid intermediate of Cys294. In turn, GSTP is hypothesized to catalyze S-glutathionylation of the sulfenic acid intermediate of Cys294 (Fig. 9G). This scenario is consistent with previous reports demonstrating that disulfide bridge formation catalyzed by PDI family enzymes results in production of H_2O_2 (6, 48), which is capable of oxidizing cysteine sulfhydrydryl (SH) to sulfenic acid (SOH) intermediates, which in turn react with GSH to form mixed disulfides or can act as a substrate for GSTP1 (32, 51).

ERp57 is known as a cofactor in assembly of the heavy chain of major histocompatibility complex class I molecules (15), regulation of calcium homeostasis, quality control of newly synthesized glycoproteins (24, 30, 43), and folding of influenza virus hemagglutinin (43). ERp57 also plays a role in hyperoxia-induced apoptosis of mouse lung endothelial cells (52). Along with PDI, ERp57 mediates misfolded protein-induced apoptosis in neuronal cells via accumulation at the ER-associated mitochondrial membrane and facilitation of oligomerization of Bak via intramolecular cysteine oxidation to form S-S bridges, leading to permeabilization of the outer membrane of mitochondria (19).

Ero1 has been identified as a key enzyme in the disulfide formation pathway and plays a role in regenerating oxidized PDI. Ero1 transfers electrons from thiol substrates, such as PDI, to molecular oxygen, producing H_2O_2 and oxidizing PDI (48). Although the present study does not confirm the requirement for Ero1 directly for increasing the oxidation state of the ER in response to Fas ligation, it is tempting to speculate that Ero1-derived H_2O_2 is responsible for the formation of a sulfenic acid intermediate (SOH) of Fas, which in turn is the target of GSTP-catalyzed S-glutathionylation. Similar to Ero1, Prx4 has also been suggested to be an alternative acceptor of electrons from PDI family enzymes (44, 45). However, results from our present study demonstrate that Prx4 was overoxidized rapidly in response to FasL, and that overexpression of Prx4 decreased Fas-SSG and apoptosis. These results suggest that excess H_2O_2 produced by rapid oxidative processing of Fas is the cause of this oxidation, instead of Prx4 being an electron acceptor in FasL-induced oxidative processing.

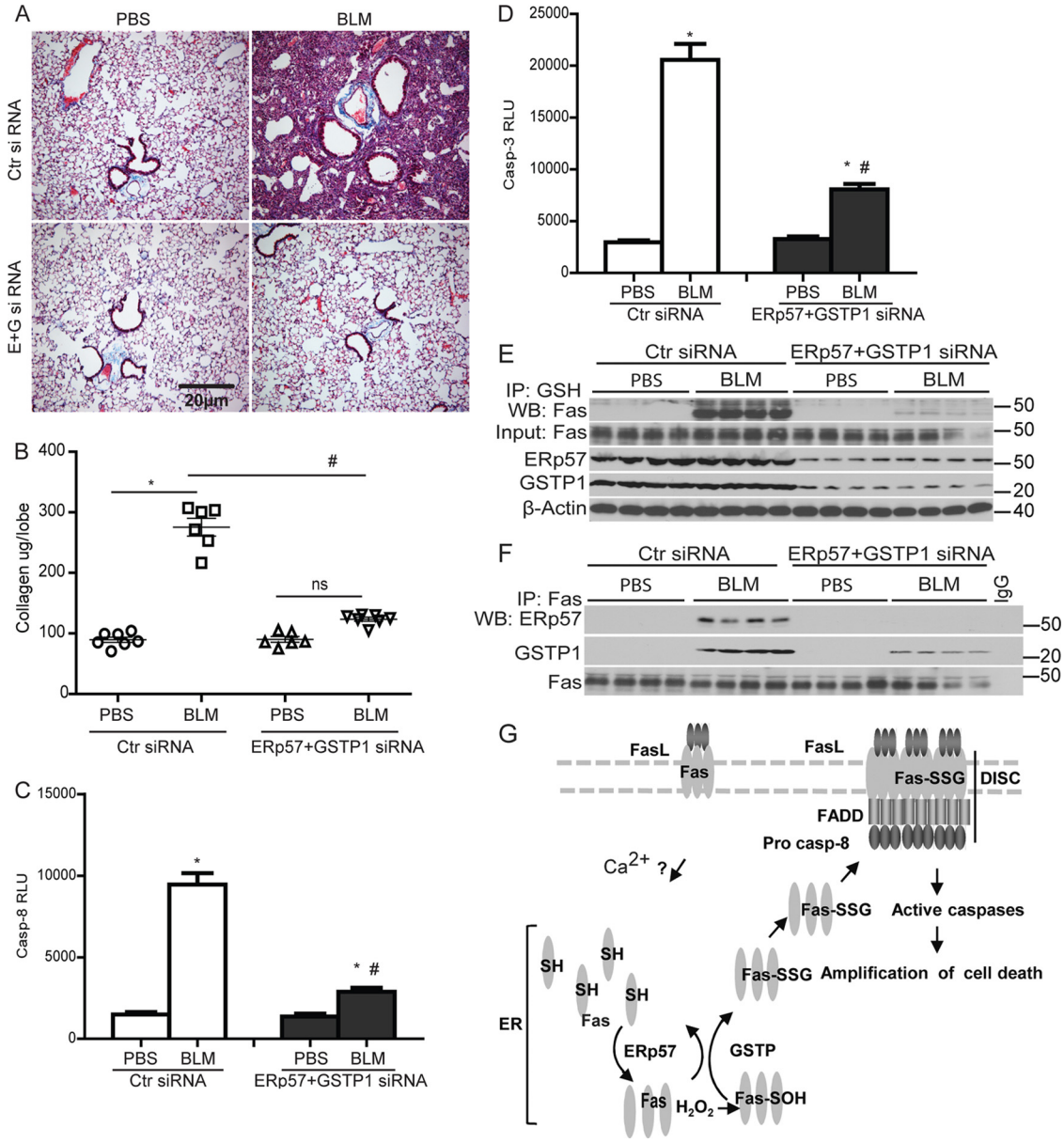

FIG 9 Knockdown of ERp57 and GSTP1 ameliorates bleomycin-induced pulmonary fibrosis in mice. C57BL/6 mice were instilled with control (Ctr) siRNA or ERp57+GSTP1 (E+G) siRNA 1 day prior to and 5 and 10 days after bleomycin (BLM) or PBS instillations. (A) Histological assessment of collagen using Masson's trichrome. (B) Quantitative assessment of collagen content in the upper right lung lobe of mice instilled with siRNAs and bleomycin or PBS by the Sircol assay. Results are expressed as μg collagen/lobe and are representative of 6 to 7 mice/group. *, $P < 0.05$ compared to PBS groups. #, $P < 0.05$ compared to BLM-Ctr siRNA-instilled mice (ANOVA). Measurement of caspase-3 (C) and -8 (D) activities in lung homogenates 15 days following instillation of PBS or BLM. *, $P < 0.05$ compared to PBS groups. #, $P < 0.05$ compared to the Ctr siRNA group (ANOVA). (E) Fas-SSG in lung tissue 15 days following instillation with bleomycin (BLM). (F) Associations between Fas, ERp57, and GSTP 15 days following instillation with BLM. Lung lysates were subjected to IP using anti-Fas antibody or IgG as a control. WB were probed for Fas, ERp57, and GSTP1. (G) Model depicting initial FasL-Fas signaling to the ER by an undetermined Ca^{2+}-dependent mechanism. FasL-triggered oxidative processing of a latent pool of Fas in the ER mediates its S-glutathionylation (Fas-SSG) via the coordinated actions of ERp57 and GSTP. This in turn increases surface Fas, promotes DISC assembly and caspase activation, and amplifies cell death.

A recent body of work has clearly demonstrated the role of GSTs as regulators of molecular pathways that control cell division and apoptosis (1, 38, 51). Interestingly, GSTP1 has been shown to glutathionylate a 1-Cys peroxiredoxin, Prx6, during its regeneration cycle via an SOH intermediate (32). Furthermore, a recent study demonstrated that *Gstp*$^{-/-}$ mouse embryonic fibroblasts showed significantly less glutathionylation of proteins during oxidative and nitrosative stress (47). Results of the present study demonstrate that FasL induced a rapid interaction of Fas with GSTP1, which initially was observed in the ER compartment where Fas-SSG occurs and subsequently in the cytosolic/plasma membrane fraction (Fig. 3C). siRNA-mediated knockdown or pharmacological inhibition of GSTP1 both resulted in decreased Fas-SSG, although not in a complete lack of S-glutathionylation.

The residual increases in Fas-SSG that are observed may be the result of incomplete knockdown or inhibition of GSTP. Alternatively, it is possible that spontaneous reaction between GSH and Fas-SOH accounts for the observed increased in S-glutathionylation of Fas in the absence of GSTP1 at the later time points. Furthermore, the enhanced ratio of glutathione disulfide to reduced glutathione present in the ER may also contribute to Fas-SSG in the absence of GSTP.

Lung fibrosis is believed to be a manifestation of dysregulated repair following injury, in association with impaired reepithelialization and aberrant myofibroblast activation and proliferation (23). Numerous pathways have been linked to the pathogenesis of fibrotic lung disease, including Fas (4, 49), which contributes to apoptosis of lung epithelial cells. A redox imbalance also has been implicated in disease pathogenesis (25), although mechanistic details whereby oxidative changes intersect with profibrotic signaling pathways remain elusive. Results from the present study demonstrate that during the pathogenesis of bleomycin-induced lung fibrosis, interactions between Fas, ERp57, and GSTP occur, together with marked increases in Fas-SSG and increased activities of caspase-3 and -8. Furthermore, we demonstrate in the present study that ERp57 and GSTP are causally linked to lung fibrogenesis induced by bleomycin, suggesting that ER-linked ERp57 and GSTP-catalyzed S-glutathionylation of Fas is a critical mechanism that drives disease pathogenesis. Worthy of mention are studies demonstrating increases in ER stress in patients with familial idiopathic pulmonary fibrosis, who have mutations in surfactant protein C (29, 46). Further studies are needed to unravel whether increased oxidative processing and S-glutathionylation of Fas occur in those patients, which could enable new therapeutic strategies to alleviate the progression of fibrosis.

ACKNOWLEDGMENTS

We thank Jessica Reiss for technical assistance, Andreas Koening and Karen Fortner for *caspase3*$^{-/-}$ and *lpr* mice, and the University of Vermont microscopy imaging facility (supported by NCRR 1S10RR019246).

This work was funded by NIH grants RO1 HL079331, HL060014, and HL085464 to Y.M.W.J.-H., NIH P30 RR 031158 (VLC-COBRE pilot investigation award) to V.A., and NCI RO1 CA85660 to K.D.T.

Y.M.W.J.-H. and V.A. have a patent application on Grx-based therapies.

REFERENCES

1. **Adler V, et al.** 1999. Regulation of JNK signaling by GSTp. EMBO J. **18**:1321–1334.
2. **Alcorn JF, et al.** 2009. c-Jun N-terminal kinase 1 is required for the development of pulmonary fibrosis. Am. J. Respir. Cell Mol. Biol. **40**:422–432.
3. **Anathy V, et al.** 2009. Redox amplification of apoptosis by caspase-dependent cleavage of glutaredoxin 1 and S-glutathionylation of Fas. J. Cell Biol. **184**:241–252.
4. **Aoshiba K, Yasui S, Tamaoki J, Nagai A.** 2000. The Fas/Fas-ligand system is not required for bleomycin-induced pulmonary fibrosis in mice. Am. J. Respir. Crit. Care Med. **162**:695–700.
5. **Appenzeller-Herzog C, Ellgaard L.** 2008. The human PDI family: versatility packed into a single fold. Biochim. Biophys. Acta **1783**:535–548.
6. **Appenzeller-Herzog C, Riemer J, Christensen B, Sorensen ES, Ellgaard L.** 2008. A novel di switch mechanism in Ero1alpha balances ER oxidation in human cells. EMBO J. **27**:2977–2987.
7. **Banner DW, et al.** 1993. Crystal structure of the soluble human 55 kd TNF receptor-human TNF beta complex: implications for TNF receptor activation. Cell **73**:431–445.
8. **Bodmer JL, Schneider P, Tschopp J.** 2002. The molecular architecture of the TNF superfamily. Trends Biochem. Sci. **27**:19–26.
9. **Boyland E, Chasseaud LF.** 1969. The role of glutathione and glutathione S-transferases in mercapturic acid biosynthesis. Adv. Enzymol. Relat. Areas Mol. Biol. **32**:173–219.
10. **Budinger GR, et al.** 2006. Proapoptotic Bid is required for pulmonary fibrosis. Proc. Natl. Acad. Sci. U. S. A. **103**:4604–4609.
11. **Coe H, Michalak M.** 2010. ERp57, a multifunctional endoplasmic reticulum resident oxidoreductase. Int. J. Biochem. Cell Biol. **42**:796–799.
12. **Degli Esposti M, et al.** 2009. Fas death receptor enhances endocytic membrane traffic converging into the Golgi region. Mol. Biol. Cell **20**:600–615.
13. **Douglas KT.** 1987. Mechanism of action of glutathione-dependent enzymes. Adv. Enzymol. Relat. Areas Mol. Biol. **59**:103–167.
14. **Franco R, Cidlowski JA.** 2009. Apoptosis and glutathione: beyond an antioxidant. Cell Death Differ. **16**:1303–1314.
15. **Garbi N, Hammerling G, Tanaka S.** 2007. Interaction of ERp57 and tapasin in the generation of MHC class I-peptide complexes. Curr. Opin. Immunol. **19**:99–105.
16. **Golan-Gerstl R, Wallach-Dayan SB, Amir G, Breuer R.** 2007. Epithelial cell apoptosis by fas ligand-positive myofibroblasts in lung fibrosis. Am. J. Respir. Cell Mol. Biol. **36**:270–275.
17. **Gross E, et al.** 2006. Generating disulfides enzymatically: reaction products and electron acceptors of the endoplasmic reticulum thiol oxidase Ero1p. Proc. Natl. Acad. Sci. U. S. A. **103**:299–304.
18. **Hengartner MO.** 2000. The biochemistry of apoptosis. Nature **407**:770–776.
19. **Hoffstrom BG, et al.** 2010. Inhibitors of protein disulfide isomerase suppress apoptosis induced by misfolded proteins. Nat. Chem. Biol. **6**:900–906.
20. **Holler N, et al.** 2003. Two adjacent trimeric Fas ligands are required for Fas signaling and formation of a death-inducing signaling complex. Mol. Cell. Biol. **23**:1428–1440.
21. **Huh JY, et al.** 2012. Peroxiredoxin 3 is a key molecule regulating adipocyte oxidative stress, mitochondrial biogenesis, and adipokine expression. Antioxid. Redox Signal. **16**:229–243.
22. **Jansens A, van Duijn E, Braakman I.** 2002. Coordinated nonvectorial folding in a newly synthesized multidomain protein. Science **298**:2401–2403.
23. **Janssen-Heininger YM, et al.** 2010. Regulation of apoptosis through cysteine oxidation: implications for fibrotic lung disease. Ann. N. Y. Acad. Sci. **1203**:23–28.
24. **Jessop CE, et al.** 2007. ERp57 is essential for efficient folding of glycoproteins sharing common structural domains. EMBO J. **26**:28–40.
25. **Kinnula VL, Fattman CL, Tan RJ, Oury TD.** 2005. Oxidative stress in pulmonary fibrosis: a possible role for redox modulatory therapy. Am. J. Respir. Crit. Care Med. **172**:417–422.
26. **Klausner RD, Donaldson JG, Lippincott-Schwartz J.** 1992. Brefeldin A: insights into the control of membrane traffic and organelle structure. J. Cell Biol. **116**:1071–1080.
27. **Klomsiri C, et al.** 2010. Use of dimedone-based chemical probes for sulfenic acid detection evaluation of conditions affecting probe incorporation into redox-sensitive proteins. Methods Enzymol. **473**:77–94.
28. **Kuwano K, et al.** 1999. Essential roles of the Fas-Fas ligand pathway in the development of pulmonary fibrosis. J. Clin. Investig. **104**:13–19.
29. **Lawson WE, et al.** 2011. Endoplasmic reticulum stress enhances fibrotic remodeling in the lungs. Proc. Natl. Acad. Sci. U. S. A. **108**:10562–10567.
30. **Li Y, Camacho P.** 2004. Ca2+-dependent redox modulation of SERCA 2b by ERp57. J. Cell Biol. **164**:35–46.
31. **Lyttle MH, et al.** 1994. Isozyme-specific glutathione-S-transferase inhibitors: design and synthesis. J. Med. Chem. **37**:189–194.
32. **Manevich Y, Feinstein SI, Fisher AB.** 2004. Activation of the antioxidant enzyme 1-CYS peroxiredoxin requires glutathionylation mediated by heterodimerization with pi GST. Proc. Natl. Acad. Sci. U. S. A. **101**:3780–3785.
33. **Mieyal JJ, Gallogly MM, Qanungo S, Sabens EA, Shelton MD.** 2008. Molecular mechanisms and clinical implications of reversible protein S-glutathionylation. Antioxid. Redox Signal. **10**:1941–1988.
34. **Peter ME, Krammer PH.** 1998. Mechanisms of CD95 (APO-1/Fas)-mediated apoptosis. Curr. Opin. Immunol. **10**:545–551.
35. **Reynaert NL, et al.** 2006. Dynamic redox control of NF-kappaB through glutaredoxin-regulated S-glutathionylation of inhibitory kappaB kinase beta. Proc. Natl. Acad. Sci. U. S. A. **103**:13086–13091.
36. **Rhee SG, Woo HA, Kil IS, Bae SH.** 2011. Peroxiredoxin as a peroxidase

for as well as a regulator and sensor of local peroxides. J. Biol. Chem. **287**:4403–4410.
37. **Salmeen A, et al.** 2003. Redox regulation of protein tyrosine phosphatase 1B involves a sulphenyl-amide intermediate. Nature **423**:769–773.
38. **Schroer KT, et al.** 2011. Downregulation of glutathione S-transferase pi in asthma contributes to enhanced oxidative stress. J. Allergy Clin. Immunol. **128**:539–548.
39. **Seo YH, Carroll KS.** 2009. Profiling protein thiol oxidation in tumor cells using sulfenic acid-specific antibodies. Proc. Natl. Acad. Sci. U. S. A. **106**: 16163–16168.
40. **Sevier CS, Kaiser CA.** 2006. Conservation and diversity of the cellular disulfide bond formation pathways. Antioxid. Redox Signal. **8**:797–811.
41. **Shrivastava P, et al.** 2004. Reactive nitrogen species-induced cell death requires Fas-dependent activation of c-Jun N-terminal kinase. Mol. Cell. Biol. **24**:6763–6772.
42. **Smith CA, Farrah T, Goodwin RG.** 1994. The TNF receptor superfamily of cellular and viral proteins: activation, costimulation, and death. Cell **76**:959–962.
43. **Solda T, Garbi N, Hammerling GJ, Molinari M.** 2006. Consequences of ERp57 deletion on oxidative folding of obligate and facultative clients of the calnexin cycle. J. Biol. Chem. **281**:6219–6226.
44. **Tavender TJ, Sheppard AM, Bulleid NJ.** 2008. Peroxiredoxin IV is an endoplasmic reticulum-localized enzyme forming oligomeric complexes in human cells. Biochem. J. **411**:191–199.
45. **Tavender TJ, Springate JJ, Bulleid NJ.** 2010. Recycling of peroxiredoxin IV provides a novel pathway for disulphide formation in the endoplasmic reticulum. EMBO J. **29**:4185–4197.
46. **Thomas AQ, et al.** 2002. Heterozygosity for a surfactant protein C gene mutation associated with usual interstitial pneumonitis and cellular nonspecific interstitial pneumonitis in one kindred. Am. J. Respir. Crit. Care Med. **165**:1322–1328.
47. **Townsend DM, et al.** 2009. Novel role for glutathione S-transferase pi. Regulator of protein S-glutathionylation following oxidative and nitrosative stress. J. Biol. Chem. **284**:436–445.
48. **Tu BP, Weissman JS.** 2002. The FAD- and O(2)-dependent reaction cycle of Ero1-mediated oxidative protein folding in the endoplasmic reticulum. Mol. Cell **10**:983–994.
49. **Wallach-Dayan SB, Golan-Gerstl R, Breuer R.** 2007. Evasion of myofibroblasts from immune surveillance: a mechanism for tissue fibrosis. Proc. Natl. Acad. Sci. U. S. A. **104**:20460–20465.
50. **Wozniak AL, et al.** 2006. Requirement of biphasic calcium release from the endoplasmic reticulum for Fas-mediated apoptosis. J. Cell Biol. **175**:709–714.
51. **Xiong Y, Uys JD, Tew KD, Townsend DM.** 2011. S-glutathionylation: from molecular mechanisms to health outcomes. Antioxid. Redox Signal. **15**:233–270.
52. **Xu D, Perez RE, Rezaiekhaligh MH, Bourdi M, Truog WE.** 2009. Knockdown of ERp57 increases BiP/GRP78 induction and protects against hyperoxia and tunicamycin-induced apoptosis. Am. J. Physiol. Lung Cell. Mol. Physiol. **297**:L44–L51.
53. **Zhang K, Kaufman RJ.** 2008. From endoplasmic-reticulum stress to the inflammatory response. Nature **454**:455–462.